

Transition from a filamentary mode to a diffuse one with varying distance from needle to stream of an argon plasma jet

Hui-Min Xu(许慧敏), Jing-Ge Gao(高敬格), Peng-Ying Jia(贾鹏英), Jun-Xia Ran(冉俊霞), Jun-Yu Chen(陈俊宇), and Jin-Mao Li(李金懋)

Citation: Chin. Phys. B, 2024, 33 (**1**): 015205. DOI: 10.1088/1674-1056/ad0149
Journal homepage: http://cpb.iphy.ac.cn; http://iopscience.iop.org/cpb

What follows is a list of articles you may be interested in

Compared discharge characteristics and film modifications of atmospheric pressure plasma jets with two different electrode geometries

Xiong Chen(陈雄), Xing-Quan Wang(王兴权), Bin-Xiang Zhang(张彬祥), Ming Yuan(袁明), and Si-Ze Yang(杨思泽)

Chin. Phys. B, 2023, 32 (**11**): 115201. DOI: 10.1088/1674-1056/ace768

Efficient hydrophilicity improvement of titanium surface by plasma jet in micro-hollow cathode discharge geometry

Peng-Ying Jia(贾鹏英), Han-Xiao Jia(贾焓潇), Jun-Xia Ran(冉俊霞), Kai-Yue Wu(吴凯玥), Jia-Cun Wu(武珈存), Xue-Xia Pang(庞学霞), and Xue-Chen Li(李雪辰)

Chin. Phys. B, 2023, 32 (**8**): 085202. DOI: 10.1088/1674-1056/acbde9

Influence of oxygen addition on the discharge characteristics of an argon plasma jet at atmospheric pressure

Junyu Chen(陈俊宇), Na Zhao(赵娜), Jiacun Wu(武珈存), Kaiyue Wu(吴凯玥), Furong Zhang(张芙蓉),Junxia Ran(冉俊霞), Pengying Jia(贾鹏英), Xuexia Pang(庞学霞), and Xuechen Li(李雪辰)

Chin. Phys. B, 2022, 31 (**6**): 065205. DOI: 10.1088/1674-1056/ac601a

Sterilization of mycete attached on the unearthed silk fabrics by an atmospheric pressure plasma jet

Rui Zhang(张锐), Jin-song Yu(於劲松), Jun Huang(黄骏), Guang-liang Chen(陈光良), Xin Liu(刘欣), Wei Chen(陈维), Xing-quan Wang(王兴权), Chao-rong Li(李超荣)

Chin. Phys. B, 2018, 27 (**5**): 055207. DOI: 10.1088/1674-1056/27/5/055207

Characteristic plume morphologies of atmospheric Ar and He plasma jets excited by a pulsed microwave hairpin resonator

Zhao-Quan Chen(陈兆权), Ben-Kuan Zhou(周本宽), Huang Zhang(张煌), Ling-Li Hong(洪伶俐), Chang-Lin Zou(邹长林), Ping Li(李平), Wei-Dong Zhao(赵卫东), Xiao-Dong Liu(刘晓东), Olga Stepanova, A A Kudryavtsev

Chin. Phys. B, 2018, 27 (**5**): 055202. DOI: 10.1088/1674-1056/27/5/055202

Transition from a filamentary mode to a diffuse one with varying distance from needle to stream of an argon plasma jet

Hui-Min Xu(许慧敏)[1], Jing-Ge Gao(高敬格)[1], Peng-Ying Jia(贾鹏英)[2,†], Jun-Xia Ran(冉俊霞)[2], Jun-Yu Chen(陈俊宇)[2], and Jin-Mao Li(李金懋)[2,3]

[1] *School of Information and Electrical Engineering, Hebei University of Engineering, Handan* 056038, *China*
[2] *College of Physics Science and Technology, Hebei University, Baoding* 071002, *China*
[3] *School of Electrical and Information Engineering, Heilongjiang University of Technology, Jixi* 158100, *China*

(Received 15 August 2023; revised manuscript received 17 September 2023; accepted manuscript online 9 October 2023)

Plasma jet has extensive application potentials in various fields, which normally operates in a diffuse mode when helium is used as the working gas. However, when less expensive argon is used, the plasma jet often operates in a filamentary mode. Compared to the filamentary mode, the diffuse mode is more desirable for applications. Hence, many efforts have been exerted to accomplish the diffuse mode of the argon plasma jet. In this paper, a novel single-needle argon plasma jet is developed to obtain the diffuse mode. It is found that the plasma jet operates in the filamentary mode when the distance from the needle tip to the central line of the argon stream (d) is short. It transits to the diffuse mode with increasing d. For the diffuse mode, there is always one discharge pulse per voltage cycle, which initiates at the rising edge of the positive voltage. For comparison, the number of discharge pulse increases with an increase in the peak voltage for the filamentary mode. Fast photography reveals that the plasma plume in the filamentary mode results from a guided positive streamer, which propagates in the argon stream. However, the plume in the diffuse mode originates from a branched streamer, which propagates in the interfacial layer between the argon stream and the surrounding air. By optical emission spectroscopy, plasma parameters are investigated for the two discharge modes, which show a similar trend with increasing d. The diffuse mode has lower electron temperature, electron density, vibrational temperature, and gas temperature compared to the filamentary mode.

Keywords: plasma jet, diffuse mode, filamentary mode, optical emission spectroscopy

PACS: 52.80.Tn, 52.50.Dg, 52.70.Kz **DOI:** 10.1088/1674-1056/ad0149

1. Introduction

Without the need for a vacuum device, atmospheric pressure plasma jet possesses the merits of low cost and easy operation.[1] More importantly, other than in a confined gap between electrodes, the plasma jet can emanate a remote plasma plume abundant with active species in open space.[2,3] Hence, the plasma jet has been extensively used in various application fields, including material synthesis,[4] surface modification,[5,6] ozone generation,[7] water purification,[8] pollutant degradation,[9] methane conversion,[6] light source,[10] sterilization,[11,12] catalysis,[13] and biomedicine,[14] *etc*.

The plasma jet composed of two naked electrodes can be driven by a radio-frequency (RF) voltage, whose plasma plume actually has a high gas temperature (much higher than room temperature).[15–17] The high temperature makes the RF plasma jet unfit for the treatment of vulnerable workpieces or biomaterials. If a dielectric layer is inserted into the two electrodes, a plasma jet in a dielectric barrier discharge (DBD) geometry is constructed. The gas temperature of the DBD plasma jet can be significantly reduced due to the intermittent discharge aspects. Then, a room-temperature plume can be easily emanated downstream of the DBD plasma jet.[18,19] The DBD plasma jet is normally fed with noble gases, such as helium, argon, neon, *etc*.[20] With helium used as the working gas, the plasma plume is diffuse with a satisfactory length.[18] Namely, a helium plasma jet operates in a diffuse mode. When less expensive argon is used, the plasma plume is often constricted to a filament.[21,22] That is, an argon plasma jet tends to operate in a filamentary mode.[23] Compared to the filamentary mode, the diffuse mode is more desirable in applications such as biomedicine and surface modification.[24] As a result, many efforts have been made to realize the diffuse mode of the argon plasma jet.

The diffuse mode is achieved when argon is mixed with some impurities, such as ammonia,[24] acetone,[25] hydrogen,[26] and ethanol.[27] The additive content needs to be controlled precisely, otherwise the diffuse mode is destroyed and will return to the filamentary one. With pure argon used as the working gas, the diffuse mode is realized outside of the plasma jet, while the filamentary mode is operated inside the jet.[28] The inner filament is thought to provide a high pre-ionization for the outside discharge, which is important for the realization of the diffuse mode. By deploying a plate electrode downstream of the plasma jet with a single needle electrode, the diffuse mode is obtained with increasing the bias voltage

†Corresponding author. E-mail: jiapengying@hbu.edu.cn

© 2024 Chinese Physical Society and IOP Publishing Ltd

applied to the plate.[23]

Inspired by the potential applications of the argon plasma jet, a novel discharge device is developed, which gives rise to the diffuse mode by varying the distance from the needle to the stream in this paper. Through visualization, optoelectrical measurement, and fast photography, the mechanism of the diffuse mode is revealed. Moreover, the plasma parameters are investigated by optical emission spectroscopy during the transition from the filamentary mode to the diffuse one.

2. Experimental setup

The schematic diagram of the experimental setup is drawn in Fig. 1.

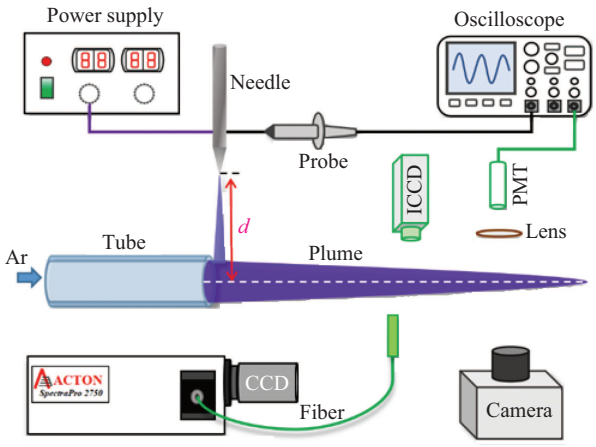


Fig. 1. Schematic diagram of the experimental setup.

The plasma jet is composed of a glass tube (inner and outer diameters of 3.0 mm and 5.0 mm, respectively) and a needle electrode (1.0 mm in diameter) with a tip radius of about 400 μm. Different to the ordinary single-needle plasma jet, whose electrode is coaxially wrapped by the tube and parallel to the working gas stream the needle in the novel plasma jet is poised outside the tube end (the jet nozzle), which is perpendicular to the gas stream. The distance from the tip of the needle to the central line of the tube is defined as d, which is an important parameter of the discharge mode of the plasma jet. The plasma jet is fed with argon with a purity of 99.99%, whose flow rate (Q) is controlled by a gas flowmeter (Sevenstar CS200A). The needle is electrically connected with the high-voltage output of a power supply (Suman CTP-2000K), which can provide a sinusoidal voltage with a frequency of 25 kHz and an amplitude (V_p) of up to 20 kV. The applied voltage (V_a) is detected by a high voltage probe (Tektronix P6015A) and then displayed by a digital oscilloscope (Tektronix DPO4104). Due to the lack of a ground electrode, it is hard to directly measure the discharge current. As an alternate approach, integrated light emission from the discharge is detected by a photomultiplier tube (PMT) (ET Enterprises 9130/100B), whose window is deployed on the image plane of a convex lens. Then, the light emission signal is simultaneously displayed by the oscilloscope with the waveform of V_a. In addition, the discharge can be recorded by a digital camera (Canon EOS 5D Mark IV) and an intensified charge coupled device (ICCD) (Intelligent Scientific System EYEITS-D-HQB-F) with different exposure times (t_{exp}). The control of the ICCD gating has been described in detail in our previous work.[29] A spectrometer (ACTON SP2750) with a grating of 2400 grooves/mm is utilized to collect the optical emission spectrum from the discharge.

3. Results and discussion

With increasing V_p higher than 15.0 kV, a plasma plume emanates from the jet nozzle. The plasma plume operates in the filamentary mode when the distance from the needle tip to the central line of the tube (d) is short, which transits to the diffuse mode when d is increased, as shown in Fig. 2. From the end-view images, it is clear that the filament is presented as a bright spot, while the diffuse plume appears as an emission ring in the periphery. Hence, it can be speculated that the discharge initiates in the argon stream for the filamentary mode, while in the interfacial layer between the argon stream and the ambient air for the diffuse mode. Besides the downstream plume, an upstream plume (corresponding to the needle-tube discharge as mentioned below) can also be observed in the filamentary mode. However, it is absent in the diffuse mode. In addition, the plasma plume in both modes elongates with increasing V_p. Under a constant V_p, the plume is longer in the filamentary mode in contrast to the diffuse one.

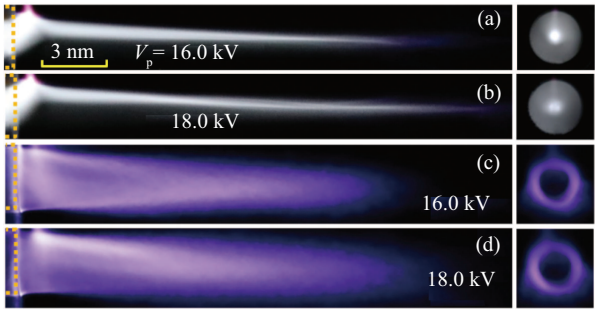


Fig. 2. Side-view (the left) and end-view (the right) images with t_{exp} of 0.1 s for the argon plume with $Q = 5.0$ L/min, $d = 5.0$ mm for panels (a) and (b), 10.0 mm for panels (c) and (d). The tube nozzle is marked as dashed lines for clarity.

Figure 3 presents waveforms of applied voltage and integrated light emission for the plasma plumes in Fig. 2. In the filamentary mode, there is one discharge per voltage cycle, which initiates at the rising edge of the positive voltage (Fig. 2(a)). The discharge number per voltage cycle increases with an increase in V_p, as shown in Fig. 2(b). Moreover, the first discharge with high V_p initiates almost at zero voltage, which is similar to the phenomenon in dielectric barrier discharge (DBD).[30] With low or high V_p, there is only one dis-

charge per voltage cycle in the diffuse mode, which always appears at the rising edge of the positive voltage (see Figs. 2(c) and 2(d)). The discharge intensity increases with the increasing V_p.

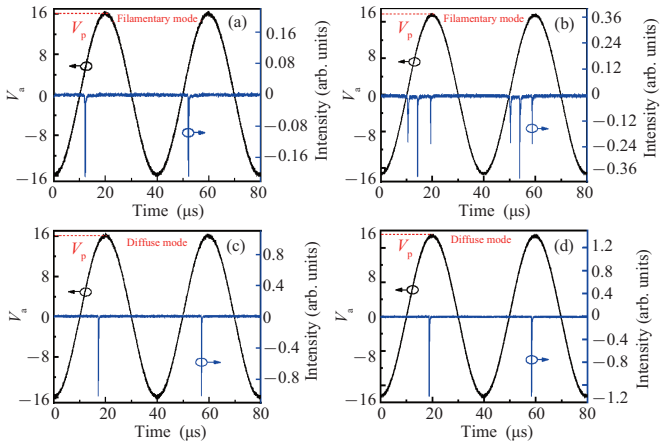


Fig. 3. Waveforms of applied voltage and integrated light signal emitted from the argon plume. Panels (a)–(d) correspond to Figs. 2(a)–2(d), respectively.

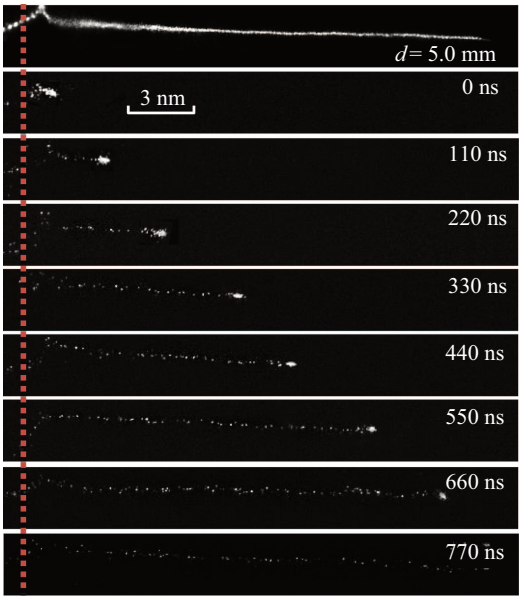


Fig. 4. Single-shot ICCD images for the argon plume operated in the filamentary mode (Fig. 2(a)). The t_{exp} of the ICCD is the whole discharge duration for the top image and 10 ns for the others.

Fast photography is implemented for the filamentary mode, as presented in Fig. 4. One can see from the top image that the discharge between the needle and the tube (the needle-tube discharge) is striated, while the streamer is continuous. The phenomenon of striation is also observed in DBD.[31] Due to the great difference in mobility between electrons and positive ions, electrons drift toward and enter the needle anode in the needle-tube discharge, depositing positive ions in the discharge channel and on the inner surface of the tube.[32] With the proceeding of the needle-tube discharge, more and more positive ions are accumulated, which can enhance the electric field in the right region of the needle. As a result, the electric field grows with time, inducing a positive streamer when it reaches a threshold. Hence, an emission layer (plasma bullet) appears near the tip of the needle at 0 ns. Then, the plasma bullet, also referred to as streamer head, propagates away from the needle tip in the downstream region from 110 ns to 770 ns. It can also be called a guided streamer owing to the constant propagation direction. In addition to the bright streamer head, weak emission can also be discerned in the channel behind the streamer head. At 770 ns, the head of the guided streamer reaches the plume tail and then the discharge quenches. Hence, it can be concluded that the filamentary mode originates from the propagation of the guided streamer in the argon stream.

Figure 5 presents temporal evolution of the argon plume in the diffuse mode. It can be found that the needle-tube discharge is almost absent in this mode. The positive streamer originally propagating in the air reaches the vicinity of the interfacial layer between the argon stream and the ambient air at 0 ns. Due to penning ionization between argon and nitrogen,[33] the breakdown threshold in the interfacial layer is lower than that in the argon stream. As a result, other than in the argon stream, the streamer tends to propagate in the interfacial layer under this condition. Moreover, the streamer is branched in the layer. As time elapses from 60 ns to about 420 ns, the branched streamer propagates in the interfacial layer toward the plume end. Behind the bright streamer heads, the emission in the channel is hardly discernible. From Fig. 5, one can see that the position and number of the streamer head are random. Hence, it can be concluded that the diffuse mode results from the propagation of the randomly branched streamer in the interfacial layer. In other words, the diffuse plume corresponds to the temporal superposition of branched streamers.[34]

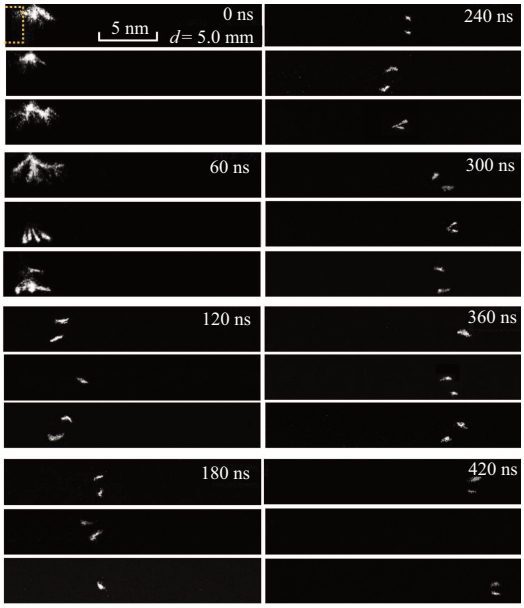


Fig. 5. Single-shot ICCD images with t_{exp} of 10 ns for the argon plume operated in the diffuse mode (Fig. 2(c)). Due to the randomness of the discharge, three images are given in a column for a given moment.

Optical emission spectra are compared in Fig. 6 for the two modes of the argon plasma jet. The spectra are clearly dominated by Ar atomic lines (Ar I ($4p \rightarrow 4s$)) in the red spectral region (690 nm–800 nm). In the blue spectral region, the spectra are rich in molecular rotational and vibrational bands, for instance, the hydroxyl band ($A^2\Sigma^+ \rightarrow X^2\Pi$) of OH, and the second positive system band ($C^3\Pi_u \rightarrow B^3\Pi_g$) of N_2. In fact, the spectra shown in Fig. 6 have been normalized at 763 nm. By comparing the spectra emitted from the two modes, one can see that the molecular vibrational band of N_2 in the diffuse mode has a stronger intensity than in the filamentary mode. The presence of the second positive system band ($C^3\Pi_u \rightarrow B^3\Pi_g$) of N_2 is attributed to the diffusion of air into argon.[35] Obviously, compared to the argon stream in which the streamer propagates in the filamentary mode, the interfacial layer in which the streamer propagates in the diffuse mode has a higher air content. Resultantly, the intensity of N_2 ($C^3\Pi_u \rightarrow B^3\Pi_g$) is higher in the diffuse mode in contrast to that in the filamentary mode.

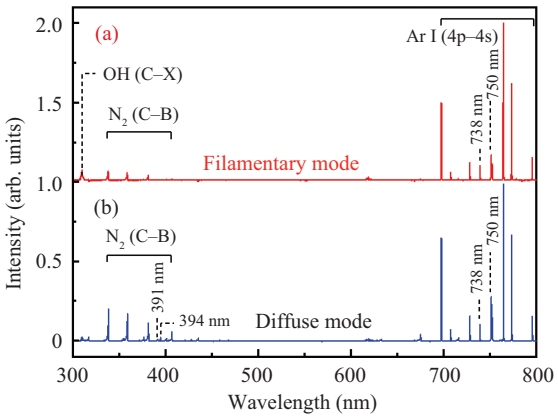


Fig. 6. The scanned spectra for 300 nm–800 nm (normalized at 763 nm) emitted from the argon plume in the filamentary mode (a) and the diffuse mode (b). Panels (a) and (b) correspond to Figs. 2(a) and 2(c), respectively.

The $N_2^+(B^2\Sigma_g^+)$ is mainly populated through collisions with electrons above 18.7 eV, whereas N_2 is primarily excited to $N_2(C^3\Pi_u)$ via collisions with electrons above 11 eV.[36] Hence, higher electron temperature (T_e) results in more population of $N_2^+(B^2\Sigma_g^+)$ compared to that of $N_2(C^3\Pi_u)$. The de-excitation process of the two excited-state species produces spontaneous radiation, corresponding to spectral lines at 391 nm and 394 nm, respectively. That is to say, the more population of $N_2^+(B^2\Sigma_g^+)$ than that of $N_2(C^3\Pi_u)$ leads to a higher intensity ratio of 391 nm to 394 nm. Therefore, T_e is represented by the intensity ratio of 391 nm to 394 nm.[34,37–39] According to the collisional-radiative model, the electron density (n_e) is related to the population ratio (n_1/n_2) of the excited states of Ar at the 2p energy level.[40] In addition, the intensity (I) of a spectral line in atmospheric pressure argon plasma can be expressed as a function of the population (n) as follows:[41]

$$\frac{I_1}{I_2} = \frac{A_1 n_1}{A_2 n_2}. \tag{1}$$

For n_1 and n_2, the Einstein coefficients A_1 and A_2 are constants. Therefore, the intensity ratio (I_1/I_2) is is positively related to the population ratio (n_1/n_2), which is a function of n_e. As a result, the intensity ratio of 738 nm to 750 nm is used as an indicator of n_e.[42,43]

By this method, T_e and n_e are investigated as functions of d, as shown in Fig. 7. It is clear that with increasing d, T_e first increases, and then decreases. On average, T_e is higher in the filamentary mode than in the diffuse mode. In addition, with varying d, n_e presents a trend similar to that of T_e. Moreover, the filamentary mode has a higher n_e than the diffuse mode. In other words, both T_e and n_e are higher in the filamentary mode than in the diffuse mode.

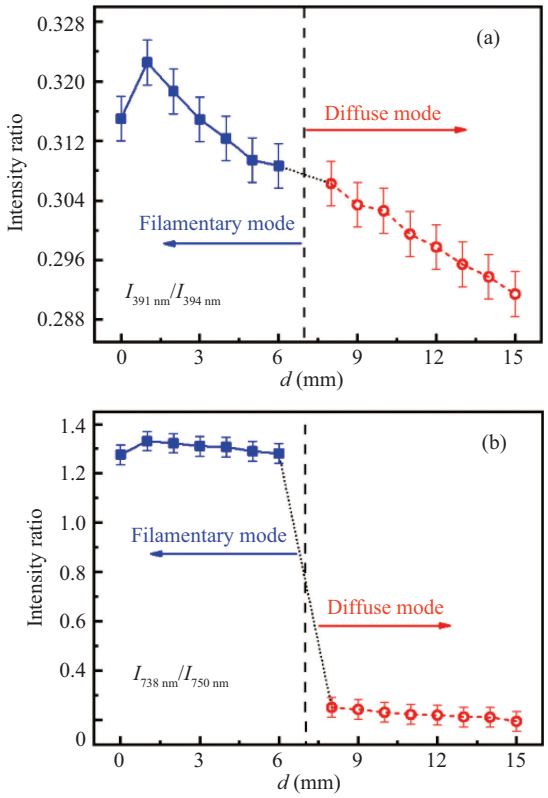


Fig. 7. Intensity ratio of the spectral lines for 391 nm to 394 nm (a) and 738 nm to 750 nm (b) as a function of d. $Q = 5.0$ L/min and $V_p = 16$ kV.

As mentioned before, in addition to the downstream streamer, there is a needle-tube discharge between the glass tube (virtual electrode) and the needle tip, which deposit positive ions in the discharge channel and on the inner surface of the tube. These spatial charges enhance the electric field to direct the streamer propagation in the downstream region. As a result, the electric field will be enhanced more severely if the needle-tube discharge is stronger. The distance between the needle to the tube end decreases with increasing d from 0 mm to 1.5 mm, which means that the gap width of the needle-tube discharge decreases accordingly. The decreasing gap width tends to initiate a stronger needle-tube discharge. Accordingly, the stronger needle-tube discharge results in a higher field with increasing d from 0 mm to 1.5 mm. Electrons in the streamer

can obtain higher energy under a higher electric field. Resultantly, T_e increases with increasing d from 0 mm to 1.5 mm. Moreover, a higher electric field corresponds to a higher α (the first Townsend ionization coefficient), which means more electrons are produced in the plasma. Therefore, n_e increases with increasing d from 0 mm to 1.5 mm. With further increasing d, the needle-tube discharge turns weaker due to the lengthening gap width. Moreover, the applied field of the needle weakens in the argon stream with increasing d ($\geq$ 1.5 mm). The two abovementioned reasons mutually lead to the weakening field of the downstream streamer with increasing d ($\geq$ 1.5 mm). As a result, T_e and n_e decrease with increasing d ($\geq$ 1.5 mm). Compared to the streamer propagating in the argon stream of the filamentary mode, there is a higher oxygen content in the interfacial layer in which the streamer propagates in the diffuse mode. Oxygen molecules can attach electrons to form negative ions,[44] resulting in a remarkable reduction of n_e.[45] As a result, n_e in the diffuse mode is remarkably lower than in the filamentary mode.

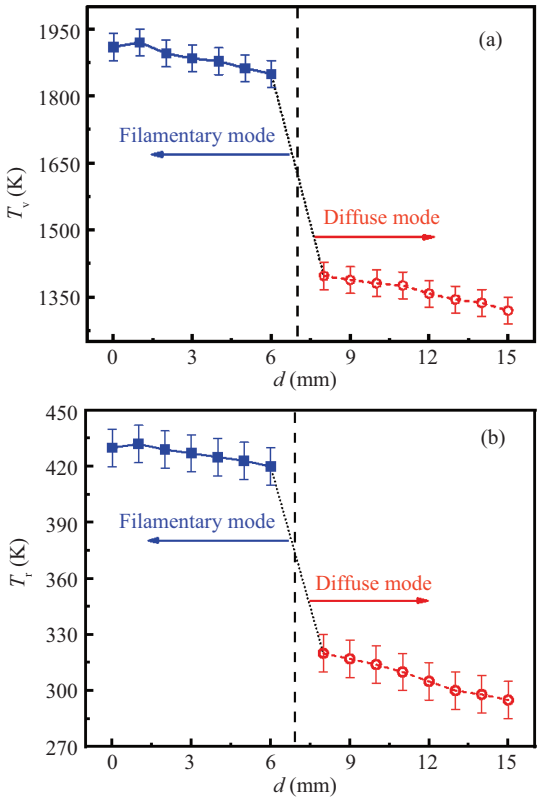


Fig. 8. The T_v (a) and T_r (b) as functions of d. $Q = 5.0$ L/min and $V_p = 16$ kV.

In addition, the vibrational temperature (T_v) can be estimated via Boltzmann plot from N_2 ($C^3\Pi_u \rightarrow B^3\Pi_g$).[20,46] Furthermore, the rotational temperature (T_r) can be diagnosed by fitting the experimental data of the first negative system (band head at 391 nm) of N_2^+.[47] The calculated results of T_v and T_r are indicated as functions of d as shown in Fig. 8. It can be found that, compared to those in the diffuse mode, the vibrational temperature T_v and the rotational temperature T_r are higher in the filamentary mode. The higher T_v and T_r in the filamentary mode come from the higher T_e and n_e. With more energetic electrons in the filamentary mode, more energy is transferred to neutral particles through collisions, leading to higher T_v and T_r.

4. Conclusions

In this paper, a novel plasma jet has been developed with a single needle perpendicular to the argon stream. Through increasing the distance d between the needle and the stream, it is found that the diffuse mode has been realized. Compared to the diffuse mode, the plasma plume is longer in the filamentary mode under a constant V_p. Waveforms of the applied voltage and the integrated light emission indicate that there is only one discharge per voltage cycle for the diffuse mode, which initiates at the rising edge of positive voltage. Distinctively, the discharge number increases with an increase in V_p for the filamentary mode. Fast photography verifies the existence of the needle-tube discharge in the filamentary mode, which accumulates positive charges in the discharge channel and on the tube inner surface to enhance the electric field. The enhanced field induces the guided positive streamer near the needle tip, which propagates in the argon stream. For the diffuse mode, the branched streamer is induced, which propagates in the interfacial layer due to penning ionization. In addition, the molecular vibrational system of N_2 has a higher intensity in the diffuse mode in contrast to the filamentary mode. However, the diffuse mode has lower T_e, n_e, T_v, and T_r values than the filamentary mode. Then, the difference of these plasma parameters in the two modes is qualitatively explained based on Penning ionization and the formation of negative ions. The results mentioned above are of great significance for the wide applications of plasma jet.

Acknowledgments

Project supported by the National Natural Science Foundation of China (Grant Nos. 51977057, 11875121, and 11805013), the Natural Science Foundation of Hebei Province, China (Grant Nos. A2020201025 and A2022201036), the Funds for Distinguished Young Scientists of Hebei Province, China (Grant No. A2012201045), the Natural Science Interdisciplinary Research Program of Hebei University (Grant No. DXK202011), and the Postgraduate's Innovation Fund Project of Hebei University (Grant No. HBU2022bs004).

References

[1] Li X C, Wu J C, Jia B Y, Wu K Y, Kang P C, Zhang F R, Zhao N, Jia P Y, Wang L and Li S Z 2020 *Appl. Phys. Lett.* **117** 134102
[2] Li X C, Lin X T, Wu K Y, Ren C H, Liu R and Jia P Y 2019 *Plasma Sources Sci. Technol.* **28** 055006

[3] Lu X P and Wu S Q 2013 *IEEE Trans. Plasma Sci.* **41** 2313
[4] Mohammadzaheri M, Siahpoush V and Asgari A 2022 *Plasma Process Polym.* **19** 2200089
[5] Jia P Y, Jia H X, Ran J X, Wu K Y, Wu J C, Pang X X and Li X C 2023 *Chin. Phys. B* **32** 085202
[6] Wu J C, Wu K Y, Chen J Y, Song C H, Jia P Y and Li X C 2021 *Plasma Sci. Technol.* **23** 085504
[7] Liu Y F, Han J M, Zhang G L, Wang J L, Li M, Yang W B, Liu C Z, Li H Q and Yang S Z 2004 *Chin. Phys. Lett.* **21** 1314
[8] Wang R X, Zhang C, Liu X, Xie Q, Yan P and Shao T 2015 *Appl. Surf. Sci.* **328** 509
[9] Wu J C, Wu K Y, Ren C H, Jia P Y and Li X C 2020 *Plasma Sci. Technol.* **22** 055505
[10] Liu F W, Nie L L and Lu X P 2022 *Plasma Sci. Technol.* **24** 055408
[11] Shi Y C, Li J J, Liu H, Zuo Y G, Bai Y, Sun Z F, Ma D L and Chen G C 2015 *Chin. Phys. Lett.* **32** 088104
[12] Wu M C, Uehara S, Wu J S, Xiao Y C, Nakajima T and Sato T 2020 *J. Phys. D: Appl. Phys.* **53** 485201
[13] Li X C, Wang B, Jia P Y, Yang L W, Li Y and Chu J D 2017 *Plasma Sci. Technol.* **19** 115505
[14] Jia P Y, Chen M, Jia H X, Tan X, Ran J X, Wu K Y, Wu J C, Chen J Y, Pang X X, Li X C and Zhao N 2023 *IEEE Transactions on Radiation and Plasma Medical Sciences* **7** 203
[15] Guo Q J, Ni G H, Li L, Lin Q F, Zhao P, Meng Y D, Zhao Y J and Sui S Y 2018 *Contributions to Plasma Physics* **58** 252
[16] Sigeneger F, Schäfer J, Weltmann K D, Foest R and Loffhagen D 2016 *Plasma Process Polym.* **14** 1600112
[17] Zhang J L, Jiang K Q, Li S Z and Xia G Q 2013 *Vacuum* **88** 47
[18] Lu X P, Jiang Z H, Xiong Q, Tang Z Y, Hu X W and Pan Y 2008 *Appl. Phys. Lett.* **92** 081502
[19] Walsh J L and Kong M G 2007 *Appl. Phys. Lett.* **91** 221502
[20] Wu J C, Li X C, Ran J X, Jia H X, Wu K Y, Han G X, Liu J N, Chen J Y, Pang X X and Jia P Y 2023 *Plasma Process Polym.* **20** 2200188
[21] Chen J Y, Zhao N, Wu J C, Wu K Y, Zhang F R, Ran J X, Jia P Y, Pang X X and Li X C 2022 *Chin. Phys. B* **31** 065205
[22] Li X C, Chen J Y, Lin X T, Wu J C, Wu K Y and Jia P Y 2020 *Plasma Sources Sci. Technol.* **29** 065015
[23] Zhao N, Wu K Y, He X R, Chen J Y, Tan X, Wu J C, Ran J X, Jia P Y and Li X C 2021 *J. Phys. D: Appl. Phys.* **55** 015203
[24] Chang Z S, Yao C W, Chen S L and Zhang G J 2016 *Phys. Plasmas* **23** 093503
[25] Urabe K, Yamada K and Sakai O 2011 *Jpn. J. Appl. Phys.* **50** 116002
[26] Wu S, Lu X, Zou D and Pan Y 2013 *J. Appl. Phys.* **114** 043301
[27] Xia W J, Liu D X, Guo L, Wang W T, Xu H, Feng C, Wang X H, Kong M G and Rong M Z 2019 *Plasma Sources Sci. Technol.* **28** 125005
[28] Li J, Xu Y G, Zhang T Y, Tang J, Wang Y S, Zhao W and Duan Y X 2017 *J. Appl. Phys.* **122** 013301
[29] Wu J C, Jia P Y, Ran J X, Chen J Y, Zhang F R, Wu K Y, Zhao N, Ren C H, Yin Z Q and Li X C 2021 *Phys. Plasmas* **28** 073501
[30] Shao X J, Ma Y, Li Y X and Zhang G J 2010 *Acta Phys. Sin.* **59** 8747 (in Chinese)
[31] Li X C, Chu J D, Zhang Q, Zhang P P, Jia P Y and Geng J L 2016 *Appl. Phys. Lett.* **109** 204102
[32] Lazukin A, Chernyshev T and Krivoruchko D 2019 *Phys. Plasmas* **26** 033513
[33] Li X C, Zhang Q, Jia P Y, Chu J D, Zhang P P and Dong L F 2017 *Phys. Plasmas* **24** 033505
[34] Yang L J, Song C H, Zhao N, Zhou S, Wu J C and Jia P P 2021 *Acta Phys. Sin.* **70** 155201 (in Chinese)
[35] Abdel-Fattah E, Bazavan M and Shindo H 2015 *Phys. Plasmas* **22** 093509
[36] Kovach Y E, Garcia M C and Foster J E 2019 *IEEE Trans. Plasma Sci.* **47** 3214
[37] Paris P, Aints M, Valk F, Plank T, Haljaste A, Kozlov K V and Wagner H E 2005 *J. Phys. D: Appl. Phys.* **38** 3894
[38] Li X C, Zhao N, Fang T Z, Liu Z H, Li L C and Dong L F 2008 *Plasma Sources Sci. Technol.* **17** 015017
[39] Wu K Y, Ren C H, Jia B Y, Lin X T, Zhao N, Jia P Y and Li X C 2019 *Plasma Process Polym.* **16** 1900073
[40] Zhu X M and Pu Y K 2010 *J. Phys. D: Appl. Phys.* **43** 015204
[41] Zhu X M and Pu Y K 2010 *J. Phys. D: Appl. Phys.* **43** 403001
[42] Wu K Y, Liu J N, Wu J C, Chen M, Ran J X, Pang X X, Jia P Y, Li X C and Ren C H 2023 *High Volt.* **8** 1161
[43] Wu K Y, Wu J C, Jia B Y, Ren C H, Kang P C, Jia P Y and Li X C 2020 *Phys. Plasmas* **27** 082308
[44] Li S Z, Huang W T, Zhang J L and Wang D Z 2009 *Appl. Phys. Lett.* **94** 111501
[45] Fang Z, Shao T, Wang R X, Yang J and Zhang C 2016 *Eur. Phys. J. D* **70** 79
[46] Li X C, Chang Y Y, Jia P Y, Zhao H H, Liu R F and Di C 2013 *Spectrosc. Spect. Anal.* **33** 926
[47] Li X C, Zhou S, Gao K, Ran J X, Wu K Y and Jia P Y 2022 *IEEE Trans. Plasma Sci.* **50** 1717